

## **Supplementary Information**

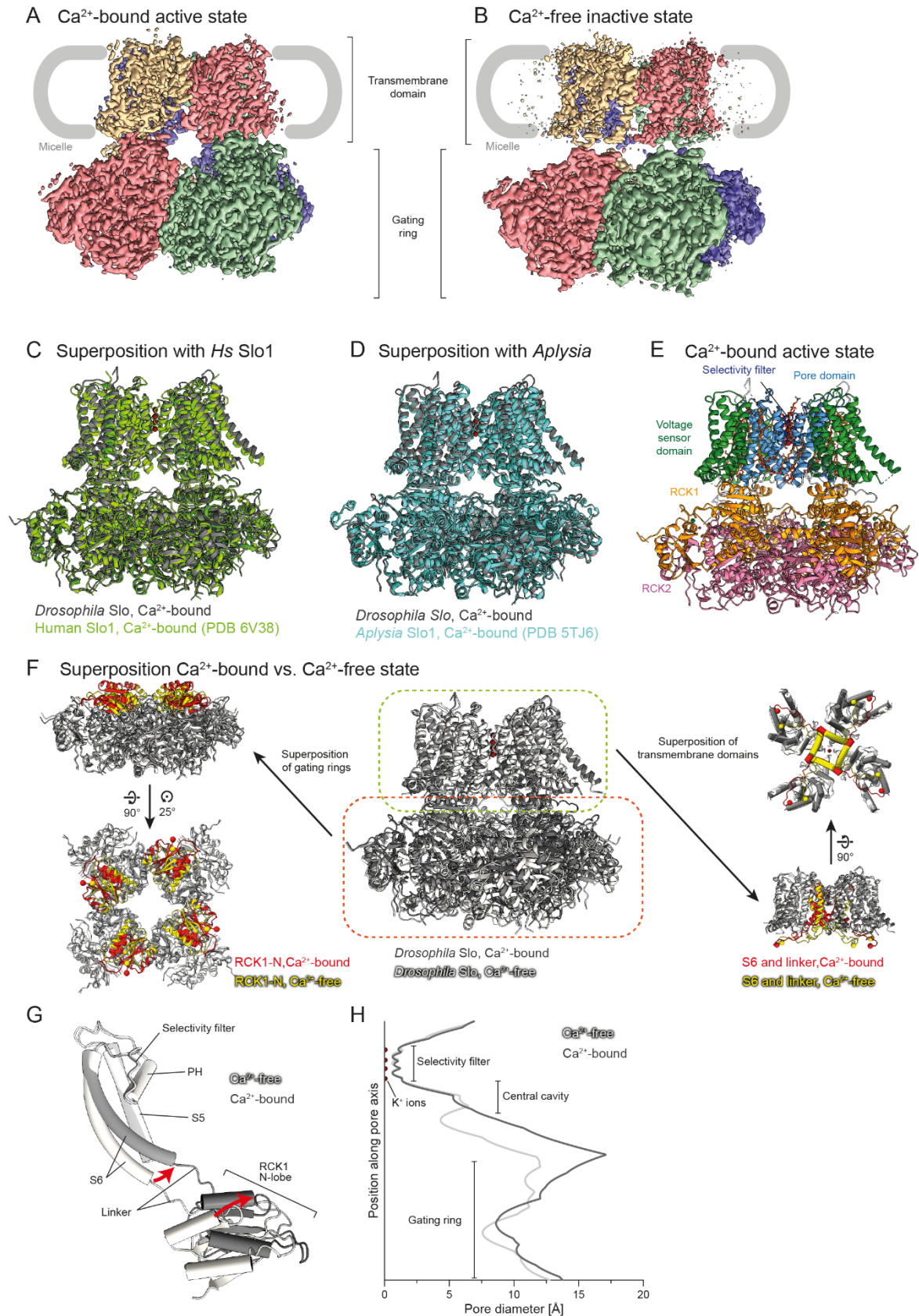
### **Small molecule modulation of the *Drosophila* Slo channel elucidated by cryo-EM**

Tobias Raisch, Andreas Brockmann, Ulrich Ebbinghaus-Kintscher, Jörg Freigang, Oliver  
Gutbrod, Jan Kubicek, Barbara Maertens, Oliver Hofnagel, Stefan Raunser

[illegible]

**Supplementary Figure 1. Sequence alignment of Slo**

Sequence alignment of metazoan Slo proteins. Amino acids which are identical between the six species are highlighted by a red background, highly conserved residues by a yellow background. Secondary structure elements as observed in our *Drosophila* Slo structure are indicated above the alignment, structural domains below the alignment. Loops and linkers which are disordered in our structures are indicated in grey. Residues involved in binding verruculogen and emodepside are highlighted by red and purple hexagons below the alignment, respectively. The gating charge residues in helix S4 are marked by blue asterisks. Amino acids involved in coordination of the  $\text{Ca}^{2+}$  and  $\text{Mg}^{2+}$  ions in the gating ring are indicated by green and purple circles, respectively. Residues lining the predicted binding pockets in *Drosophila* Slo are indicated by triangles above the alignment in the colors corresponding to Fig. 2A,B.

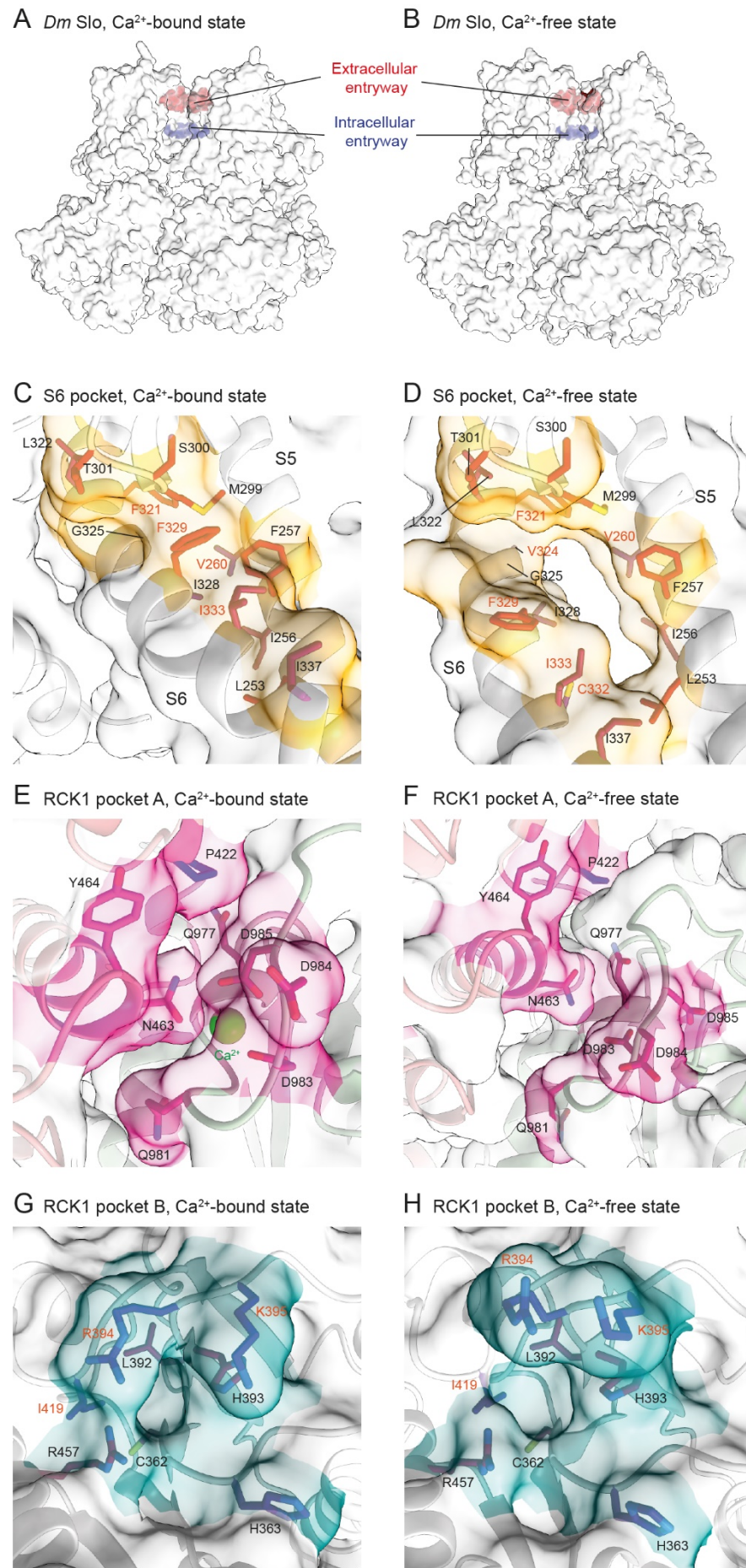


Supplementary Figure 2. Analysis of Slo apo structures

A) Cryo-EM reconstruction of  $\text{Ca}^{2+}$ -bound Slo colored by macromolecular chain as in Fig. 1C. The position of the micelle is indicated by a thick grey line.



- B) Cryo-EM reconstruction of  $\text{Ca}^{2+}$ -free Slo colored by macromolecular chain as in panel A. The position of the micelle is indicated by a thick grey line.
- C) Superposition of the  $\text{Ca}^{2+}$ -bound states of *Drosophila* Slo (grey; this work) and human Slo1 (green; PDB 6V38; <https://doi.org/10.2210/pdb6V38/pdb>).
- D) Superposition of the  $\text{Ca}^{2+}$ -bound states of *Drosophila* Slo (grey; this work) and *Aplysia* Slo1 (cyan; PDB 5TJ6; <https://doi.org/10.2210/pdb5TJ6/pdb>).
- E) Structure of Slo in the  $\text{Ca}^{2+}$ -bound active conformation shown from the side. Domains are colored according to Fig. 1A. Ions are shown as spheres ( $\text{K}^+$ : Red;  $\text{Ca}^{2+}$ : Green;  $\text{Mg}^{2+}$ : Pink). Phosphatidylcholine and cholesterol molecules are shown as sticks.
- F) Superposition of the  $\text{Ca}^{2+}$ -bound (dark grey) and  $\text{Ca}^{2+}$ -free (light grey) conformations. The panel in the center shows a global superposition. For the panels on the left side, the TMDs were omitted and the gating rings superposed to visualize the  $\text{Ca}^{2+}$ -induced movement of the RCK1 N-lobe. For the panels on the right side, the gating rings were omitted and the TMDs superposed to show the conformational change of helix S6 induced by the movement of the RCK1 N-lobe.
- G) Superposition of the pore domain and the RCK1 N-lobe in the  $\text{Ca}^{2+}$ -free (white) and  $\text{Ca}^{2+}$ -bound state (grey). As the RCK1 N-lobe shifts outwards upon  $\text{Ca}^{2+}$ -binding, it drags along the linker and kinks helix S6.
- H) Plot showing the pore diameter of the central ion conducting channel along the central fourfold axis in the  $\text{Ca}^{2+}$ -bound active (dark grey) and the  $\text{Ca}^{2+}$ -free inactive conformation (light grey). The pore is narrowest at the selectivity filter at the height of the outer leaflet of the membrane. Large changes of pore diameter are observed below the central cavity where the conformational change of helix S6 leads to a strong expansion of pore diameter. The positions of the  $\text{K}^+$  ions in the selectivity filter are indicated by red half-circles.



**Supplementary Figure 3. Surface analysis of *Drosophila* Slo**

- A) Surface representation of the  $\text{Ca}^{2+}$ -bound conformation of Slo with the intracellular entryway highlighted in blue and the extracellular entryway shown in red. Targeting these entryways to the selectivity filter would allow physical block of  $\text{K}^+$  translocation, but the chemical nature and high conservation of these sites would make design of specific and potent small molecules very challenging.
- B) Surface representation of the  $\text{Ca}^{2+}$ -free conformation of Slo with the intracellular entryway highlighted in blue and the extracellular entryway shown in red.
- C) Close-up view of the S6 pocket location in the  $\text{Ca}^{2+}$ -bound active conformation. The pocket is completely closed and buried by the shifted helix S6.
- D) Close-up view of the S6 pocket in the  $\text{Ca}^{2+}$ -free inactive conformation. The shape of the pocket is indicated as a yellow surface. Amino acid side chains that line the pocket are shown in stick representation and colored according to conservation from blue (low conservation) to red (high conservation). Residues which are identical between *Drosophila* Slo and human Slo1 are labelled with black labels, residues which differ with orange labels.
- E) Close-up view of RCK1 pocket A in the  $\text{Ca}^{2+}$ -bound active conformation. The shape of the pocket is indicated as a pink surface. Amino acid side chains that line the pocket are shown in stick representation and colored according to conservation from blue (low conservation) to red (high conservation). The pocket coincides with the inter-subunit  $\text{Ca}^{2+}$ -binding site and is highly conserved. All involved side chains are identical between *Drosophila* Slo and human Slo1.
- F) Close-up view of RCK1 pocket A in the  $\text{Ca}^{2+}$ -free inactive conformation. The shape of the pocket is very different from the  $\text{Ca}^{2+}$ -bound conformation.
- G) Close-up view of RCK1 pocket B in the  $\text{Ca}^{2+}$ -bound active conformation. The shape of the pocket is indicated as a cyan surface. Amino acid side chains that line the pocket are shown in stick representation and colored according to conservation from blue (low conservation) to red (high conservation). Residues which are identical between *Drosophila* Slo and human Slo1 are labelled with black labels, residues which are not identical with orange labels.
- H) Close-up view of RCK1 pocket B in the  $\text{Ca}^{2+}$ -free inactive conformation. The shape of the pocket is very different from the  $\text{Ca}^{2+}$ -bound conformation.

## A RCK2 pocket

	474	486	823	832	857	866	1036	1048
<i>Dm</i>	LMQYHNKAYLLNI	[...]	SPLIGLRNLV	[...]	IRREWKMLQN	[...]	ELELILAEAGSLR	
<i>Px</i>	LMQYHNKAYLLNI	[...]	SPLIGLRNLV	[...]	IRREWKMLQN	[...]	ELELILAEAGSLR	
<i>Ag</i>	LMQYHNKAYLLNI	[...]	SPLIGLRNLV	[...]	IRREWKMLQN	[...]	ELELILAEAGSLR	
<i>Aa</i>	LMQYHNKAYLLNI	[...]	SPLIGLRNLV	[...]	IRREWKMLQN	[...]	ELELILAEAGSLR	
<i>Ap</i>	LMQYHNKAYLLNI	[...]	SPLIGLRNLV	[...]	IRREWKMLQN	[...]	ELELILAEAGSLR	
<i>Am</i>	LMQYHNKAYLLNI	[...]	SPLIGLRNLV	[...]	IRREWKMLQN	[...]	ELELILAEAGSLR	
<i>Sg</i>	LMQYHNKAYLLNI	[...]	SPLIGLRNLV	[...]	IRREWKMLQN	[...]	ELELILAEAGSLR	
<i>Hs</i>	MLQYHNKAHLNI	[...]	SALIGLRNLV	[...]	LKREWETLHN	[...]	ELEALTAENALR	
<i>Mm</i>	MLQYHNKAHLNI	[...]	SALIGLRNLV	[...]	LKREWETLHN	[...]	ELEALTAENALR	
<i>Cg</i>	MLQYHNKAHLNI	[...]	SALIGLRNLV	[...]	LKREWETLHN	[...]	ELEALTAENALR	
<i>Om</i>	MLQYHNKAHLNI	[...]	SALIGLRNLV	[...]	LKREWETLHN	[...]	ELEALTAENALR	
<i>Se</i>	MLQYHNKAHLNI	[...]	SALIGLRNLV	[...]	LKREWETLHN	[...]	ELEALTAENALR	
<i>Xl</i>	MLQYHNKAHLNI	[...]	SALIGLRNLV	[...]	LKREWETLHN	[...]	ELEALTAENALR	
<i>Sh</i>	LLQYHNKAYLLNS	[...]	APLIGLRNLV	[...]	LQREWSNTAN	[...]	ALEQWLAEGGLD	
<i>Cs</i>	LLQYHNKAYLLNS	[...]	APLIGLRNLV	[...]	LQREWSNTAN	[...]	ALEQWLAEGGLD	
<i>Wb</i>	LMQYHNKAYLLNI	[...]	SPLIGLRNLV	[...]	LKREWETLHN	[...]	ELELILAEAGSLR	
<i>Bm</i>	LMQYHNKAYLLNI	[...]	SPLIGLRNLV	[...]	LKREWETLHN	[...]	ELELILAEAGSLR	
<i>Ll</i>	LMQYHNKAYLLNI	[...]	SPLIGLRNLV	[...]	LKREWETLHN	[...]	ELELILAEAGSLR	

## B RCK1 pocket A

	420	424	460	467	975	987
<i>Dm</i>	MNEID	[...]	SIKNYSDD	[...]	NVQFLDQDDDDDP	
<i>Px</i>	MNEID	[...]	SIKNYSDD	[...]	NVQFLDQDDDDDP	
<i>Ag</i>	MNEID	[...]	SIKNYSDD	[...]	NVQFLDQDDDDDP	
<i>Aa</i>	MNEID	[...]	SIKNYSDD	[...]	NVQFLDQDDDDDP	
<i>Ap</i>	MNEID	[...]	SIKNYSDD	[...]	NVQFLDQDDDDDP	
<i>Am</i>	MNEID	[...]	SIKNYSDD	[...]	NVQFLDQDDDDDP	
<i>Sg</i>	MNEID	[...]	SIKNYSDD	[...]	NVQFLDQDDDDDP	
<i>Hs</i>	LNPID	[...]	SIKNYHPK	[...]	NVQFLDQDDDDDP	
<i>Mm</i>	LNPID	[...]	SIKNYHPK	[...]	NVQFLDQDDDDDP	
<i>Cg</i>	LNPID	[...]	SIKNYHPK	[...]	NVQFLDQDDDDDP	
<i>Om</i>	LNPID	[...]	SIKNYHPK	[...]	NVQFLDQDDDDDP	
<i>Se</i>	LNPID	[...]	SIKNYHPK	[...]	NVQFLDQDDDDDP	
<i>Xl</i>	LNPID	[...]	SIKNYHPK	[...]	NVQFLDQDDDDDP	
<i>Sh</i>	MDNID	[...]	AVKNYASH	[...]	NIHYLDQDDKLSG	
<i>Cs</i>	MDNID	[...]	AVKNYASH	[...]	NIHYLDQDDKLSG	
<i>Wb</i>	MDSID	[...]	SIKNYSDD	[...]	NVQFLDQDDDDDP	
<i>Bm</i>	MDSID	[...]	SIKNYSDD	[...]	NVQFLDQDDDDDP	
<i>Ll</i>	MDSID	[...]	SIKNYSDD	[...]	NVQFLDQDDDDDP	

## C RCK1 pocket B

	360	367	390	397	415	421	455	459
<i>Dm</i>	VVCGHITY	[...]	VFLHRKPP	[...]	FOGTIMN	[...]	IMRVI	
<i>Px</i>	VVCGHITY	[...]	VFLHRKPP	[...]	FOGTIMN	[...]	IMRVI	
<i>Ag</i>	VVCGHITY	[...]	VFLHRKPP	[...]	FOGTIMN	[...]	IMRVI	
<i>Aa</i>	VVCGHITY	[...]	VFLHRKPP	[...]	FOGTIMN	[...]	IMRVI	
<i>Ap</i>	VVCGHITY	[...]	VFLHRKPP	[...]	FOGTIMN	[...]	IMRVI	
<i>Am</i>	VVCGHITY	[...]	VFLHRKPP	[...]	FOGTIMN	[...]	IMRVI	
<i>Sg</i>	VVCGHITY	[...]	VFLHRKPP	[...]	FOGTIMN	[...]	IMRVI	
<i>Hs</i>	VVCGHITL	[...]	VFLHNISP	[...]	YQGSVLN	[...]	IMRVI	
<i>Mm</i>	VVCGHITL	[...]	VFLHNISP	[...]	YQGSVLN	[...]	IMRVI	
<i>Cg</i>	VVCGHITL	[...]	VFLHNISP	[...]	YQGSVLN	[...]	IMRVI	
<i>Om</i>	VVCGHITL	[...]	VFLHNISP	[...]	YQGSVLN	[...]	IMRVI	
<i>Se</i>	VVCGHITL	[...]	VFLHNISP	[...]	YQGSVLN	[...]	IMRVI	
<i>Xl</i>	VVCGHITL	[...]	VFLHNISP	[...]	YQGSVLN	[...]	IMRVI	
<i>Sh</i>	VVCGHITL	[...]	VFLHNISP	[...]	YQGSVLN	[...]	IMRVI	
<i>Cs</i>	VVCGHITL	[...]	VFLHNISP	[...]	YQGSVLN	[...]	IMRVI	
<i>Wb</i>	VVCGHITY	[...]	VFLHRVPP	[...]	FSGTVMD	[...]	IMRVI	
<i>Bm</i>	VVCGHITY	[...]	VFLHRVPP	[...]	FSGTVMD	[...]	IMRVI	
<i>Ll</i>	VVCGHITY	[...]	VFLHRVPP	[...]	FSGTVMD	[...]	IMRVI	

## D S6 pocket

	251	262	297	303	319	339
<i>Dm</i>	AQLVSIFISVWL	[...]	VTMSTVG	[...]	VFFLLVGLAMFASISPEIIDL	
<i>Px</i>	AQLVSIFISVWL	[...]	VTMSTVG	[...]	VFFLLVGLAMFASISPEIIDL	
<i>Ag</i>	AQLVSIFISVWL	[...]	VTMSTVG	[...]	VFFLLVGLAMFASISPEIIDL	
<i>Aa</i>	AQLVSIFISVWL	[...]	VTMSTVG	[...]	VFFLLVGLAMFASISPEIIDL	
<i>Ap</i>	AQLVSIFISVWL	[...]	VTMSTVG	[...]	VFFLLVGLAMFASISPEIIDL	
<i>Am</i>	AQLVSIFISVWL	[...]	VTMSTVG	[...]	VFFLLVGLAMFASISPEIIDL	
<i>Sg</i>	AQLVSIFISVWL	[...]	VTMSTVG	[...]	VFFLLVGLAMFASISPEIIDL	
<i>Hs</i>	VNLLSIFISTWL	[...]	VTMSTVG	[...]	VFFLLVGLAMFASISPEIIDL	
<i>Mm</i>	VNLLSIFISTWL	[...]	VTMSTVG	[...]	VFFLLVGLAMFASISPEIIDL	
<i>Cg</i>	VNLLSIFISTWL	[...]	VTMSTVG	[...]	VFFLLVGLAMFASISPEIIDL	
<i>Om</i>	VNLLSIFISTWL	[...]	VTMSTVG	[...]	VFFLLVGLAMFASISPEIIDL	
<i>Se</i>	VNLLSIFISTWL	[...]	VTMSTVG	[...]	VFFLLVGLAMFASISPEIIDL	
<i>Xl</i>	VNLLSIFISTWL	[...]	VTMSTVG	[...]	VFFLLVGLAMFASISPEIIDL	
<i>Sh</i>	COLCTIFISVWL	[...]	VTMSTVG	[...]	SILFILFALATFASATPEIIVDM	
<i>Cs</i>	COLCTIFISVWL	[...]	VTMSTVG	[...]	SILFILFALATFASATPEIIVDM	
<i>Wb</i>	TQLLSIFISVCL	[...]	VTMSTVG	[...]	VFFLLVGLAMFASISPEIIDL	
<i>Bm</i>	TQLLSIFISVCL	[...]	VTMSTVG	[...]	VFFLLVGLAMFASISPEIIDL	
<i>Ll</i>	TQLLSIFISVCL	[...]	VTMSTVG	[...]	VFFLLVGLAMFASISPEIIDL	

## E Species and accession numbers

	Species	Accession numbers
<i>Dm</i>	<i>Drosophila melanogaster</i>	Fruit fly
<i>Px</i>	<i>Plutella xylostella</i>	Cabbage moth
<i>Ag</i>	<i>Anopheles gambiae</i>	African malaria mosquito
<i>Aa</i>	<i>Aedes aegypti</i>	Yellow fever mosquito
<i>Ap</i>	<i>Acyrtosiphon pisum</i>	Pea aphid
<i>Am</i>	<i>Apis mellifera</i>	Honey bee
<i>Sg</i>	<i>Schistocerca gregaria</i>	Desert locust
<i>Hs</i>	<i>Homo sapiens</i>	Human
<i>Mm</i>	<i>Mus musculus</i>	Mouse
<i>Cg</i>	<i>Cricetulus griseus</i>	Chinese hamster
<i>Om</i>	<i>Oncorhynchus mykiss</i>	Rainbow trout
<i>Se</i>	<i>Sitta europaea</i>	Eurasian nuthatch
<i>Xl</i>	<i>Xenopus laevis</i>	Western clawed frog
<i>Sh</i>	<i>Schistosoma haematobium</i>	Blood fluke
<i>Cs</i>	<i>Clonorchis sinensis</i>	Chinese liver fluke
<i>Wb</i>	<i>Wuchereria bancrofti</i>	Roundworm
<i>Bm</i>	<i>Brugia malayi</i>	Filarial nematode worm
<i>Ll</i>	<i>Loa loa</i>	Eye worm

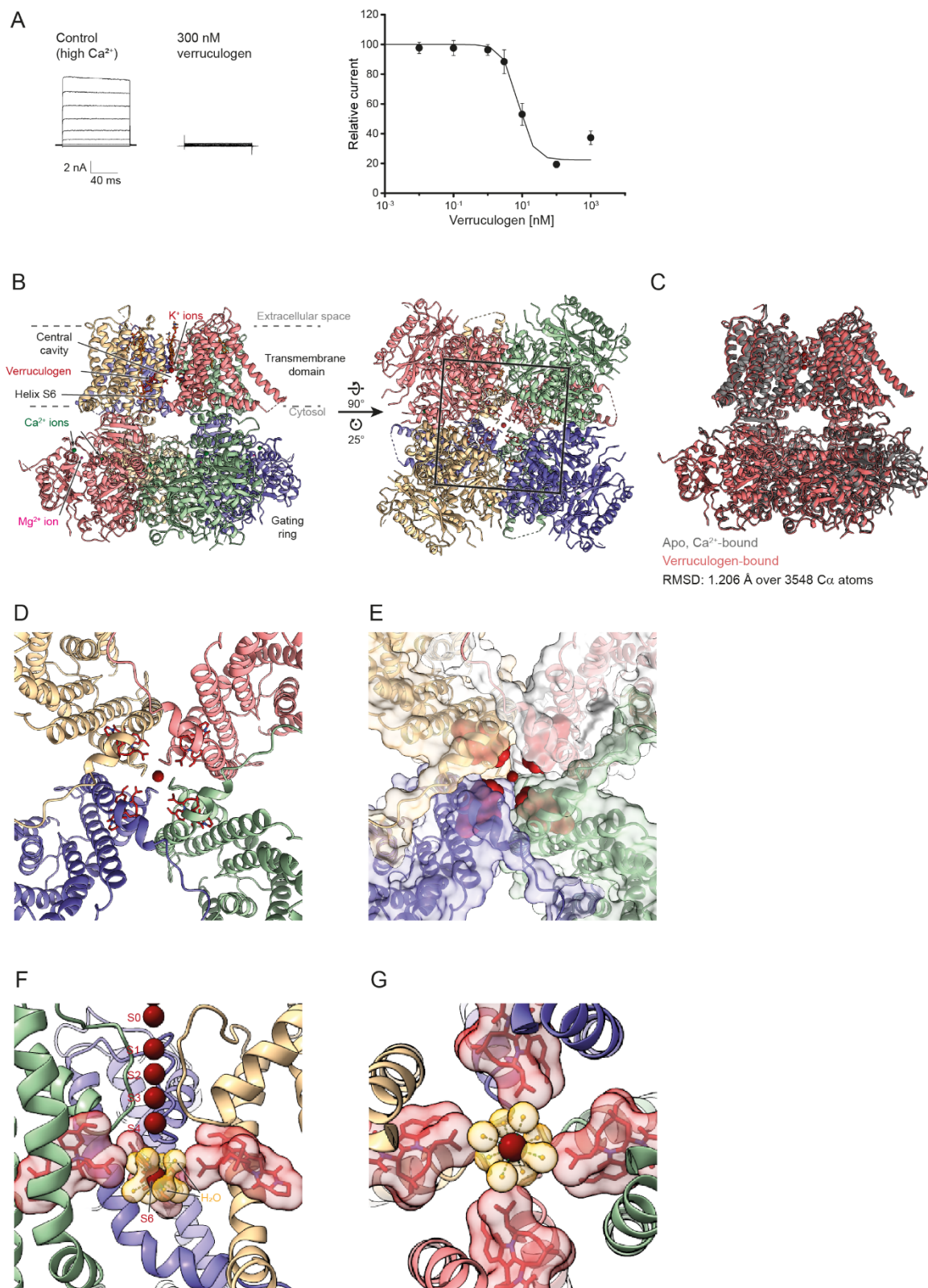
## Supplementary Figure 4. Sequence alignments of potentially druggable pockets

A) - D) Sequence alignments of amino acids lining the four pockets identified by BiteNet, i.e. the RCK2 pocket (A), the RCK1 pocket A (B), the RCK1 pocket B (C) and the S6 pocket (D), including insect, vertebrate and helminth species. Residue numbers above the alignments correspond to *Drosophila* Slo. Residues which line the pockets involving their side chains are highlighted in the colors assigned to the respective pockets in Fig. 2A,B, residues which contribute only by their main chain are indicated by a grey background. Pocket-lining residues of insect species that deviate from the *Drosophila* sequence and might therefore give rise to structural differences of the pockets between these insects are marked by green boxes.



Residues which differ between vertebrate and insect species and might allow design of insect-specific Slo modulators are highlighted by red boxes. Amino acids of helminth species that deviate from mammalian Slo and could be utilized for development of novel anthelmintics are indicated by blue boxes. Red and purple hexagons below the cavity pocket alignment in panel **B** indicate residues interacting with verruculogen and emodepside, respectively, and a purple box marks deviations from the consensus sequence in several nematode species outside the cavity-lining residues which might affect emodepside binding.

- E) List of species used in the alignments in panels **A-D**, including (from left to right) the used abbreviation, the Latin and English species names and the Uniprot or NCBI accession numbers.

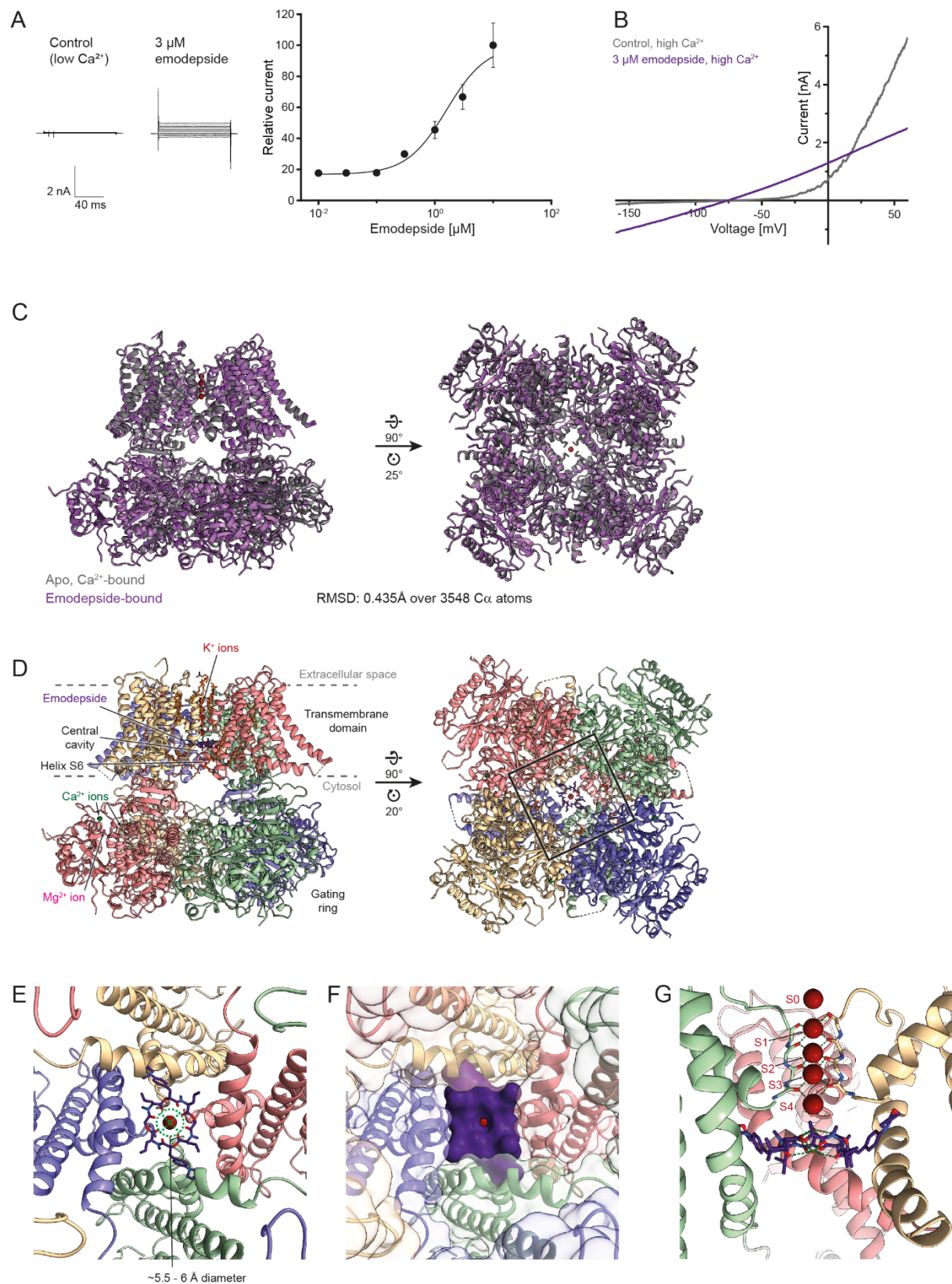


**Supplementary Figure 5. Structure of verruculogen-bound Slo**

A) Inhibition of Slo conductance by verruculogen. The left panels show representative current traces of CHO cells stably expressing Slo in presence and absence of 300 nM verruculogen under high  $\text{Ca}^{2+}$  conditions. Traces are shown for subsequent 100 ms measurements at membrane potentials between -120 and +60mV in 10mV increments. The right panel shows the

dose-response curve for verruculogen on Slo. Data points represent the mean  $\pm$  s.e. of  $n = 8$ -13 cells (selected automatically by the PatchControl384PE software; exact numbers and values are provided in the Source Data File).

- B) Cartoon representation of verruculogen-bound Slo in two orientations with colors assigned by macromolecular chain. Verruculogen is displayed as red sticks.
- C) Superposition of the  $\text{Ca}^{2+}$ -bound apo structure (grey) and the verruculogen-bound structure of *Drosophila* Slo (salmon).
- D) View from the gating ring (omitted for unobstructed view) into the central cavity and onto the selectivity filter illustrating how the aliphatic tail of verruculogen reaches into the cavity.
- E) The same view with semi-transparent surfaces of the four Slo monomers shown, as well as verruculogen as solid red surfaces illustrating the constriction of the central cavity entry by the S6 helices and by verruculogen.
- F) View of the verruculogen-bound cavity shown from the side, analogously to Fig. 4B. One of the four macromolecular chains was omitted to allow an unobstructed view into the internal pore. The three remaining protein chains are shown in cartoon representation. Verruculogen is shown as sticks and semi-transparent surface. The four  $\text{K}^+$  ions in the selectivity filter are displayed as red spheres. A hydrated  $\text{K}^+$  ion was modelled in the S6 position by superposing a KscA structure determined under high-potassium conditions (PDB 1K4C; <https://doi.org/10.2210/pdb1K4C/pdb>; Zhou et al., 2001) and is shown as spheres and semi-transparent surface.
- G) The same structural model including superposed hydrated  $\text{K}^+$  as in panel F viewed from the gating ring, showing that the constriction of pore diameter by verruculogen would make  $\text{K}^+$  reaching the selectivity filter unlikely.



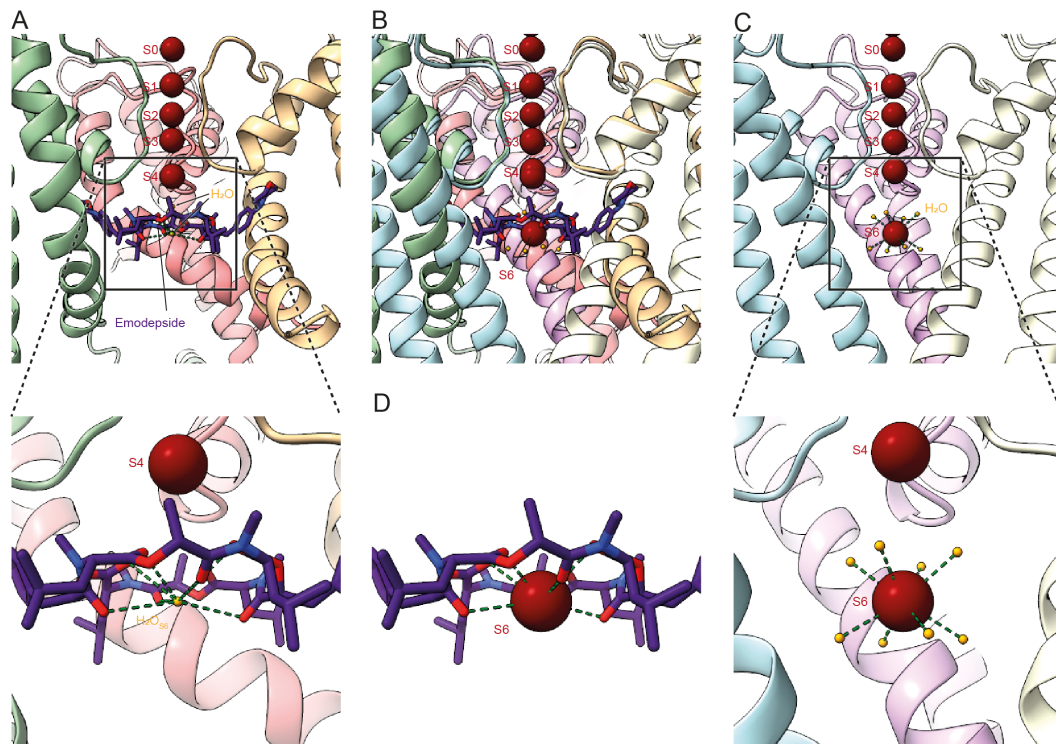
**Supplementary Figure 6. Structure of emodepside-bound Slo**

A) Activation of Slo conductance by emodepside at low  $\text{Ca}^{2+}$  concentration. The left panels show representative current traces of CHO cells stably expressing Slo before and after application of 3  $\mu\text{M}$  emodepside under low  $\text{Ca}^{2+}$  conditions. Traces are shown for subsequent 100 ms



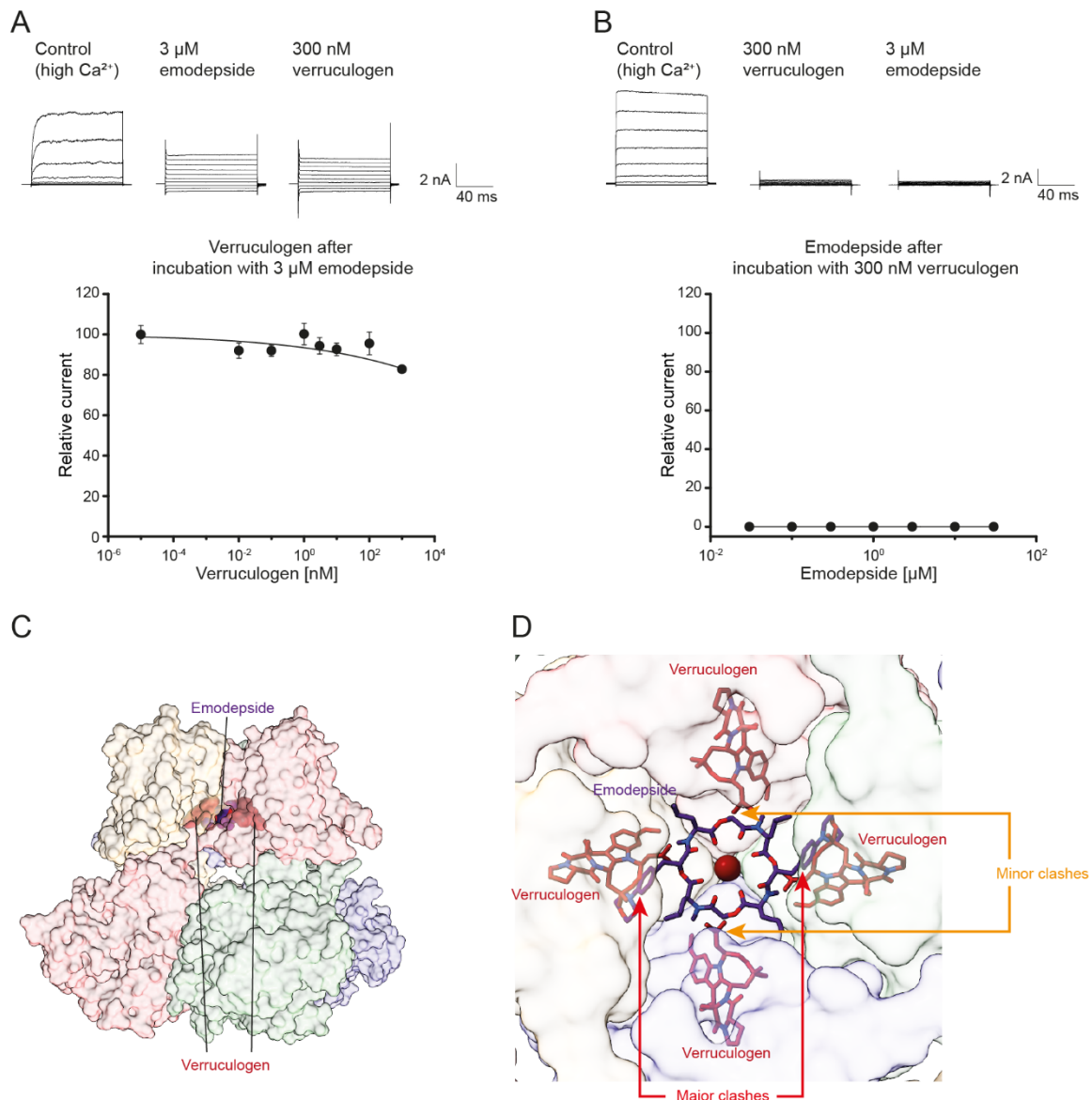
measurements at membrane potentials between -120 and +60mV in 10mV increments. The right panel shows the dose-response curve for emodepside on Slo. Data points represent the mean  $\pm$  s.e. of  $n = 12-16$  cells (selected automatically by the PatchControl384PE software; exact numbers and values are provided in the Source Data File).

- B) Current-voltage relationship of Slo in absence and presence of emodepside under high free intracellular  $\text{Ca}^{2+}$  concentration. Whole cell currents were elicited by applying voltage ramps from -160 mV to 100 mV within 170 ms. The holding potential was clamped to -100 mV.
- C) Superposition of the  $\text{Ca}^{2+}$ -bound apo structure (grey) and the emodepside-bound structure of *Drosophila* Slo (purple).
- D) Cartoon representation of emodepside-bound Slo in two orientations with colors assigned by macromolecular chain. Emodepside is displayed as purple sticks.
- E) View from the gating ring (omitted for unobstructed view) into the central cavity and onto the selectivity filter illustrating how emodepside serves as an additional ring limiting the access to the selectivity filter. The distances of opposite carbonyls in emodepside of  $\sim 5.5-6$  Å is slightly larger compared to the carbonyls in the selectivity filter ( $\sim 4.5$  Å) and might pose an explanation for the reduced conductivity of emodepside-bound Slo compared to the apo situation under high  $\text{Ca}^{2+}$  conditions.
- F) The same view with semi-transparent surface of the four Slo monomers shown, as well as emodepside as solid purple surfaces illustrating how emodepside constricts the pore diameter directly above the selectivity filter.
- G) View of the emodepside-bound Slo central cavity shown from the side. One of the four macromolecular chains was omitted to allow an unobstructed view into the internal pore. The three remaining protein chains are shown in cartoon representation. Emodepside is shown as sticks. The four  $\text{K}^{+}$  ions in the selectivity filter and the two water molecules above and below emodepside are displayed as red spheres. Hydrogen bonds between the  $\text{K}^{+}$  ions and the carbonyl oxygens of the selectivity filters of two of the four subunits, as well as hydrogen bonds between the carbonyl oxygens of emodepside and the water molecules are shown as dashed lines.



**Supplementary Figure 7. Emodepside is located perfectly to stabilize  $K^+$  in the cavity**

- A) View of the emodepside-bound cavity shown from the side, analogously to Fig. 5B. One of the four macromolecular chains was omitted to allow an unobstructed view into the internal pore. The three remaining protein chains are shown in cartoon representation. Emodepside is shown as sticks. The four  $K^+$  ions in the selectivity filter are displayed as red spheres. A water molecule (yellow sphere) was modelled into a weak density in a central position slightly beneath the emodepside ring. This water is in a position where it could be weakly coordinated by the eight carbonyl oxygens of emodepside (green dashed lines).
- B) Same representation as in panel A including a superposed crystal structure of the bacterial potassium channel KscA under high-potassium conditions (PDB 1K4C; <https://doi.org/10.2210/pdb1K4C/pdb>; Zhou et al., 2001).
- C) Same representation as in panels A and B, but only KscA is shown. In addition to the four  $K^+$  ions in the selectivity filter and one in the position S0 on the exterior side, another  $K^+$  in the S6 position inside the central cavity is fully hydrated by eight water molecules.
- D) Superposition of emodepside bound to Slo with the  $K^+$  in the S6 position of KscA. The geometry of emodepside would allow to coordinate the  $K^+$  ion in a similar but slightly distorted manner compared to a hydration shell.



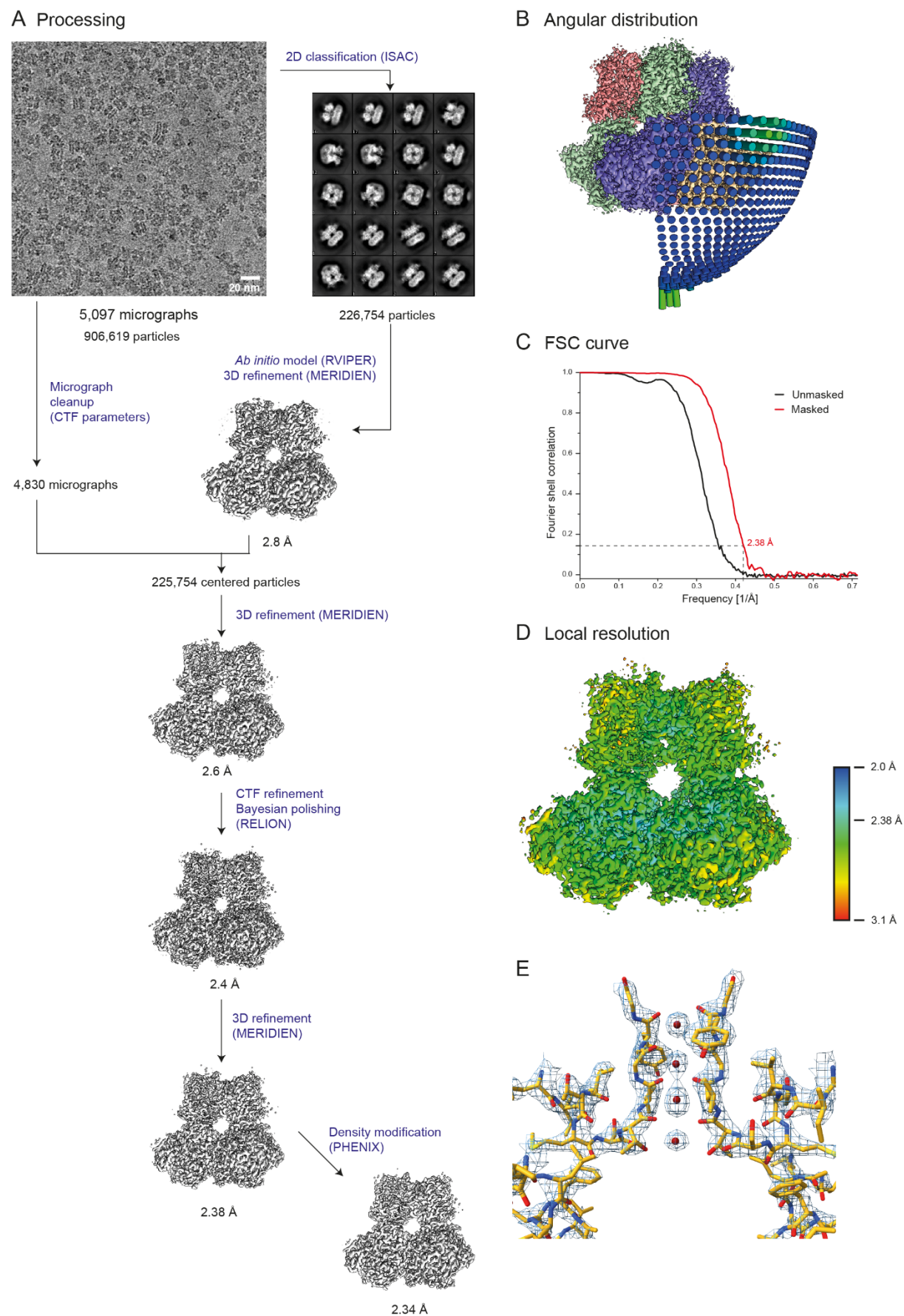
**Supplementary Figure 8. Emodepside and verruculogen compete for Slo-binding**

- A) Emodepside-bound Slo is insensitive to verruculogen inhibition. The top panels show representative whole cell currents of CHO cells expressing Slo before (left) and after exposure to 3  $\mu\text{M}$  emodepside (middle), and after subsequent exposure to 300 nM verruculogen (right). Traces are shown for subsequent 100 ms measurements at membrane potentials between -120 and +60mV in 10mV increments at a holding potential of -100mV. The lower panel shows the dose-response curve for verruculogen on Slo after application of 3  $\mu\text{M}$  emodepside. Data points represent the mean  $\pm$  s.e. of  $n = 7-11$  cells (selected automatically by the PatchControl384PE software; exact numbers and values are provided in the Source Data File).
- B) Emodepside cannot activate verruculogen-bound Slo. The top panels show representative whole cell currents before (left) and after exposure to 300 nM verruculogen (middle), and after subsequent exposure to 3  $\mu\text{M}$  emodepside (right). Traces are shown for subsequent 100 ms measurements at membrane potentials between -120 and +60mV in 10mV increments at a

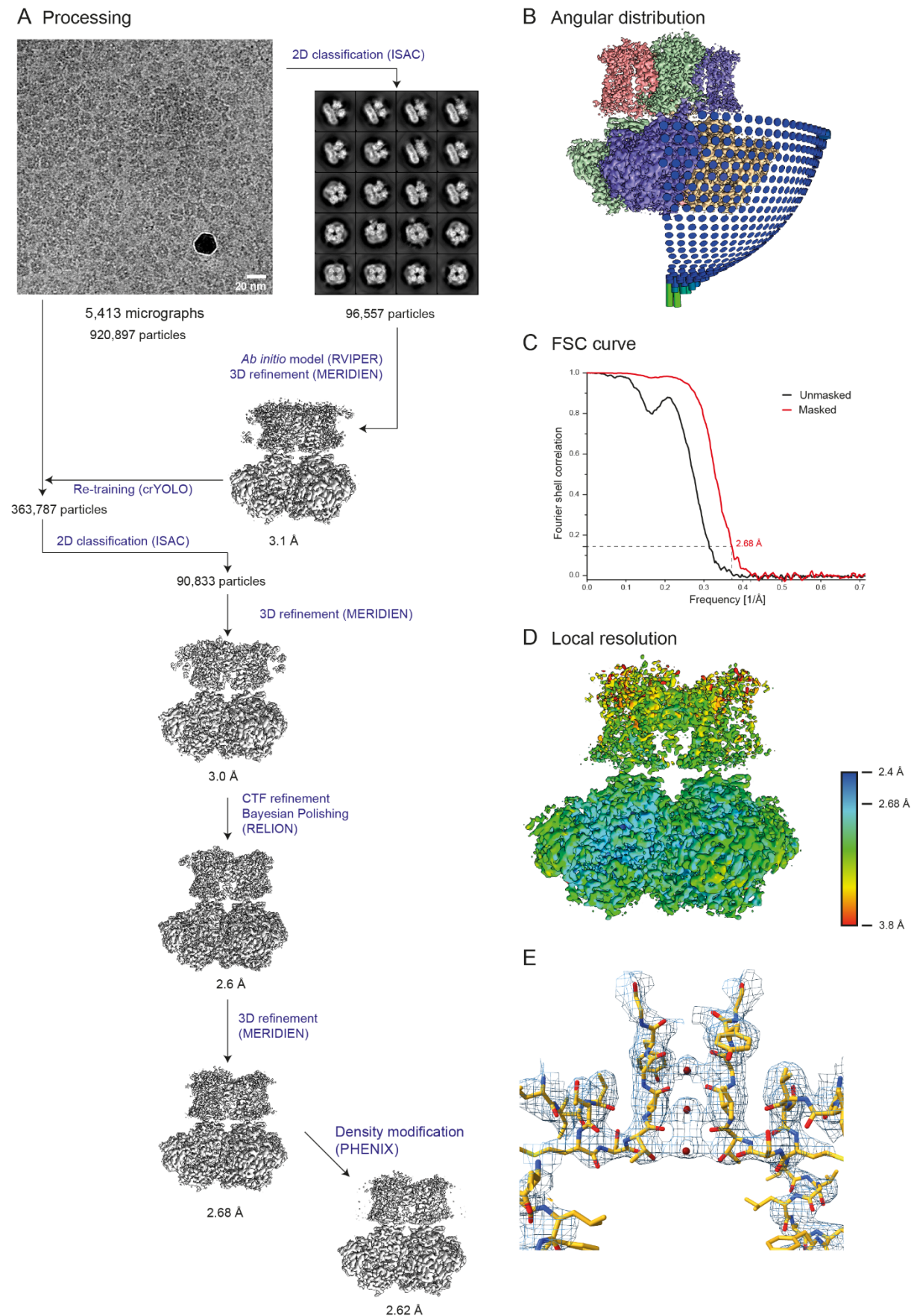
holding potential of -100mV. The lower panel shows the dose-response curve for emodepside on Slo after application of 300 nM verruculogen. Data points represent the mean  $\pm$  s.e. of n = 9-13 cells (selected automatically by the PatchControl384PE software; exact numbers and values are provided in the Source Data File).

- C) Verruculogen and emodepside bind to the same region in the central cavity close to the selectivity filter. The molecular model of Slo1 in the emodepside-bound conformation is shown from the side as a semi-transparent surface. The emodepside molecule is shown as a solid purple surface, the four superposed verruculogen molecules as red surfaces.
- D) View from the gating ring (omitted for unobstructed view) into the central cavity and onto the selectivity filter reveals clashes between emodepside and verruculogen. Slo in the emodepside-bound conformation is shown as a semi-transparent surface, the superposed Slo in the verruculogen-bound conformation omitted for clarity. Both compounds are shown in stick representation. Simultaneous binding of both compounds is precluded as the two morpholinylphenyl groups of emodepside would severely clash with verruculogen.



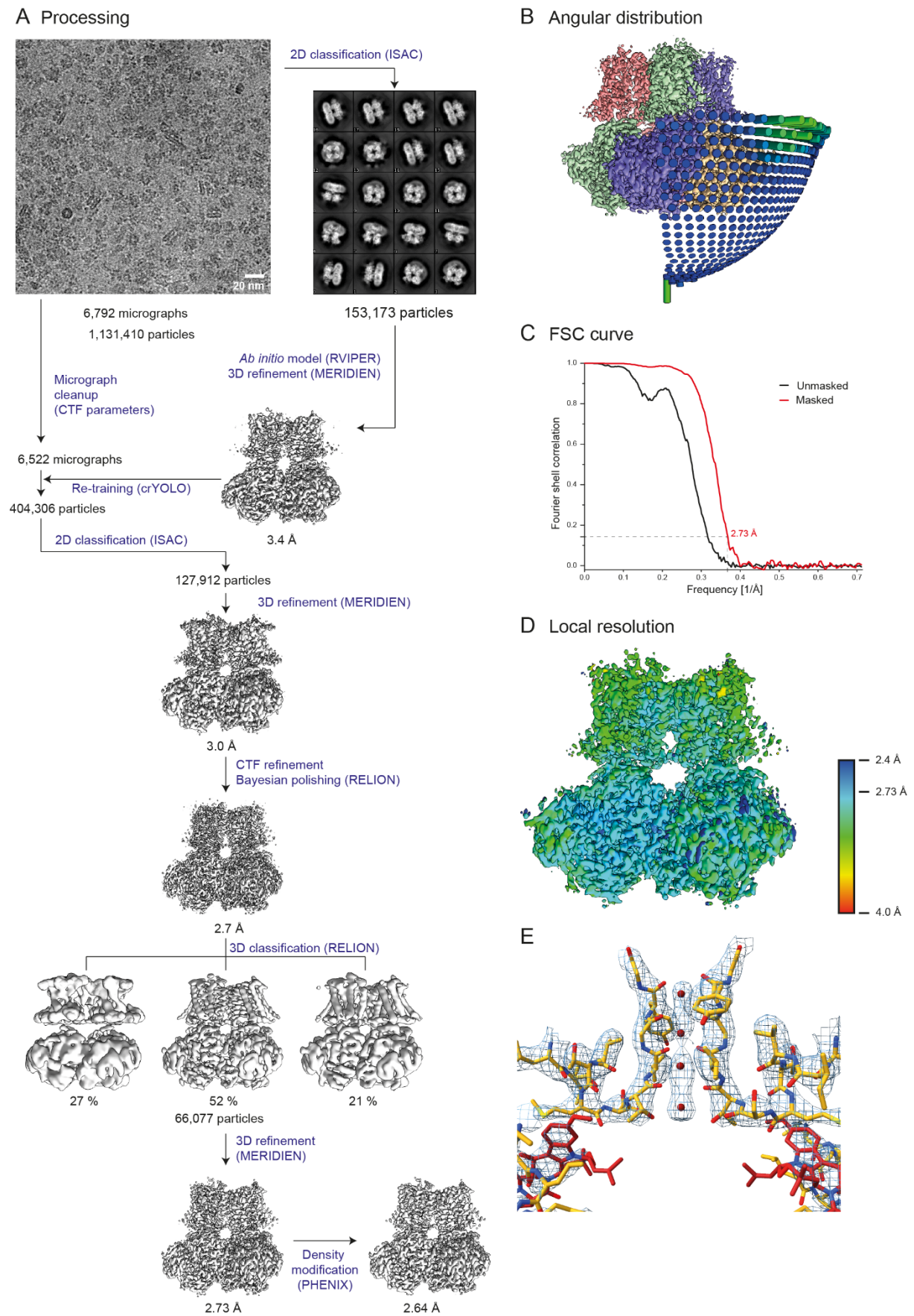
Supplementary Figure 9. Processing of  $\text{Ca}^{2+}$ -bound Slo apo EM data

- A) Processing scheme including exemplary micrograph and subset of selected 2D classes of Ca<sup>2+</sup>-bound *Drosophila* Slo.
- B) Final reconstruction of Ca<sup>2+</sup>-bound Slo. The colored bars represent angular distribution.
- C) Fourier Shell Correlation (FSC) curve between two independent half-maps reconstructed from the final set of particles. The dashed line indicates the 0.143 FSC criterion that intersects the masked FSC curve at 2.38 Å.
- D) Local resolution plotted on the final reconstruction in a rainbow-colored gradient from blue (2.0 Å) to red (3.1 Å).
- E) Experimental Coulomb potential map in the region around the selectivity filter and central cavity. For clarity, only two of the macromolecular chains are shown.

Supplementary Figure 10. Processing of  $\text{Ca}^{2+}$ -free Slo apo EM data

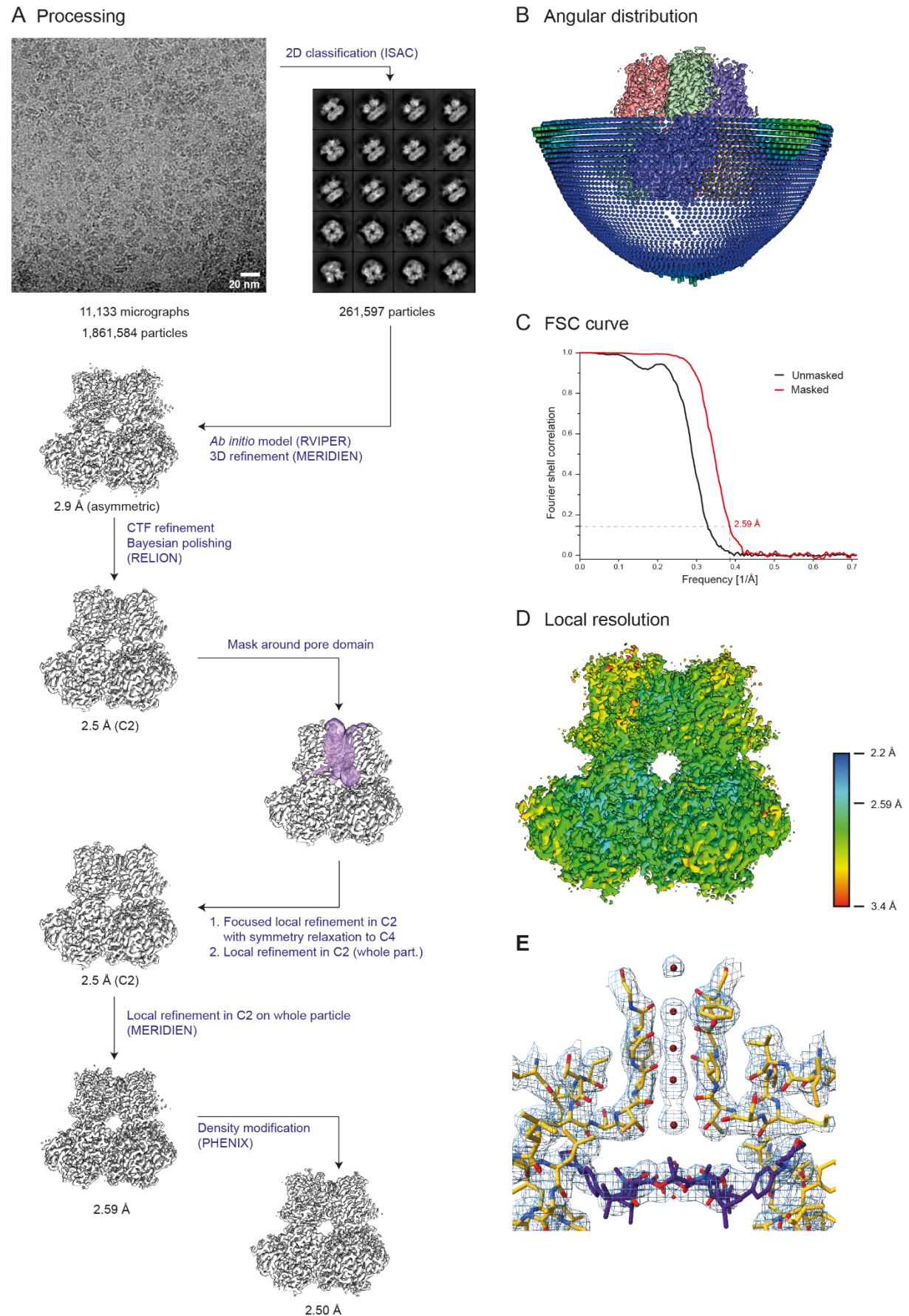
- A) Processing scheme including exemplary micrograph and subset of selected 2D classes of  $\text{Ca}^{2+}$ -free *Drosophila* Slo.
- B) Final reconstruction of  $\text{Ca}^{2+}$ -free Slo. The colored bars represent angular distribution.
- C) Fourier Shell Correlation (FSC) curve between two independent half-maps reconstructed from the final set of particles. The dashed line indicates the 0.143 FSC criterion that intersects the masked FSC curve at 2.68 Å.
- D) Local resolution plotted on the final reconstruction in a rainbow-colored gradient from blue (2.4 Å) to red (3.8 Å).
- E) Experimental Coulomb potential map in the region around the selectivity filter and central cavity. For clarity, only two of the macromolecular chains are shown.





Supplementary Figure 11. Processing of verruculogen-bound Slo EM data

- A) Processing scheme including exemplary micrograph and subset of selected 2D classes of verruculogen-bound Slo.
- B) Final reconstruction of verruculogen-bound Slo. The colored bars represent angular distribution.
- C) Fourier Shell Correlation (FSC) curve between two independent half-maps reconstructed from the final set of particles. The dashed line indicates the 0.143 FSC criterion that intersects the masked FSC curve at 2.73 Å.
- D) Local resolution plotted on the final reconstruction in a rainbow-colored gradient from blue (2.4 Å) to red (4.0 Å).
- E) Experimental Coulomb potential map in the region around the selectivity filter and central cavity. For clarity, only two of the macromolecular chains are shown.



Supplementary Figure 12. Processing of emodepside-bound Slo EM data

- A) Processing scheme including exemplary micrograph and subset of selected 2D classes of emodepside-bound Slo.
- B) Final reconstruction of emodepside-bound Slo. The colored bars represent angular distribution.
- C) Fourier Shell Correlation (FSC) curve between two independent half-maps reconstructed from the final set of particles. The dashed line indicates the 0.143 FSC criterion that intersects the masked FSC curve at 2.59 Å.
- D) Local resolution plotted on the final reconstruction in a rainbow-colored gradient from blue (2.2 Å) to red (3.4 Å).
- E) Experimental Coulomb potential map in the region around the selectivity filter and central cavity. For clarity, only two of the macromolecular chains are shown.

**Supplementary Table 1. DNA sequence of the codon-optimized Slo gene**

ATGGCTTCCGGCCTGATCGACACCAACTTCTCTTCTACCTGGCTAACGGCATGTCCGGTTGCGACCAGTCCACCGTGGGA  
 ATCTTTTGCTGACGACCTACCGACTCTCCCTTCGACGCTGACGACTGCCGTGAAAGTGCGCAAGTACTGGTGCTTCTCTGC  
 TGTCTCTATCTTACCTTCCTGGCTGGCCTGCTGGTGGTGTGCTTTGGAGGGCTTTCGCTTTCGTGTGCTGCCGTAA  
 GAGCCCCGACCTGGGTCTTAACGACCCCAAGCAGAAAGAGCAGAAAGGCTTCCCGTAACAAGCAAGAGTTCGAGGGGCACCTT  
 CATGACCGAGGCTAAGGACTGGGCTGGCGAGCTGATCTCTGGTCAAACCACCACCGGTCGTATCCTGGTGGTGTGCTGGTGT  
 TCATCTGTCTATCGCTTCCCTGATCATCTACTTCGTGGACGCTTCCCTCCGAAGAGGTCGAGCGTTGCCAGAAGTGGTCC  
 AACAACATCACCCAGCAGATCGACCTGGCCTTCAACATCTTCTTCATGGTGTACTTTTTTCATCCGCTTCATTGCCGCCTC  
 CGACAAGCTGTGGTTTATGCTCGAGATGTACTCCTTCGTCGACTACTTCACTATCCCTCCATCCTTCGTGTCCATCTACC  
 TGGACCGTACCTGGATCGGCCTGCGTTTCCTTCGTGCTCTGCGTCTGATGACCGTGCCTGACATCCTGCAGTACCTGAAC  
 GTGCTCAAGACCTCCTCCTCCATCCGTCTGGCTCAGCTGGTTTCCATCTTCATCTCCGTGTGGCTGACCGCTGCTGGTAT  
 CATCCACCTGTTGGAGAACTCTGGCGACCTCTGGACTTCGACAACGCTCACCGTCTGTCTACTGGACCTGCGTGTACT  
 TCCTGATCGTGACCATGTCTACCGTCGGTTACGGCGACGTGTACTGCGAGACTGTGCTGGGTCGTACTTTCCTCGTGTTT  
 TTCTTGCTCGTCGGCTGGCTATCTTCGCTTCTTGCATCCCCGAGATCATCGACCTGATCGGCACCCGTGCTAAGTACGG  
 TGGCACCTGAAGAACGAGAAGGGTCGTCGTACATCGTCGTGTGCGGTACATCACCTACGAGTCCGTGTCTCACTTCC  
 TGAAGGATTTCTTGCACGAGGACCGCGAGGACGTGGACGTGGAAGTTGTGTCTTGCACCGCAAGCCTCCAGACCTGGAA  
 CTCGAGGACTGTTCAAGCGCCACTTACCACCGTCGAGTTCTTCCAGGGAACCATCATGAACCTATCGACCTGCAGCG  
 TGTGAAGGTGCACGAAGTGAAGCTTGGCTGGTGTGGCTAACAACTACTGTGACGACCCGACGCTGAGGACGCTGCTA  
 ACATCATGCGTGTGATCTCCATCAAGAACTACTCCGACGACATCCGCGTGATCATCCAGTGATGCAGTACCACAACAAG  
 GCCTACCTGCTGAACATCCCATCTGGGACTGGAAGCAAGCGCAGCAGTGATCTGCCTGGCTGAGCTGAAGCTGGGTTT  
 CATTGCTCAGTCTTGCTGGCTCCTGGTTCTCCACCATGATGGCTAACCTGTTTCGCTATGCGCTCCTTCAAGACTTCCC  
 CTGACATGCAGTCTTGACCAACGACTACCTGCGTGGCACCGCATGGAAATGTACACCGAGACTCTGTCCCCAACCTTC  
 ATCGGTATCCCTTTTCGCTCAGGCTACCGAGCTGTGCTTCTCCAAGCTCAAGCTGCTGCTGCTGCTATCGAGATCAAGGG  
 TGCTGAGGAAGGTGCTGACTCCAAGATCTCTATCAACCCTCGTGGTGTAGATCCAGGCTAACACCCAGGGATTCTTTA  
 TCGCTCAGTCCGCTGACGAAGTGAAGCGCGCTGGTTCTACTGCAAGGCTTGCCACGAGGATATCAAGGACGAAACCTG  
 ATCAAGAAATGCAAGTGCAAAAACCTGGCCACCTTCCGCAAGGGTGTCCGTGCTGTTCAAATGGTCGGACGCGCTTCTGA  
 CATCACCCGTGACAGAGAGGACACCAACCTGCTCAACCGTAACGTGCGTGTCCCAACGGTACTGGAAACGGCACTGGTG  
 GCATGCACCACATGAACAACACAGCTGCTGCCGCTGCAGTGCAGTGTGCGGGAAAGCAAGTGAACAAAGTGAAGCCC  
 ACCGTGAACGTGTCCCGTCAGGTTGAGGGTCAAGTGATCTCCCTAGCCAGTACAACCGTCTACCTCTCGTTCTCCGG  
 TACTGGCACCCAAAACGAGAACGGCGGTGTCTCTGCCCCGTGGTATCGCTGACGATCAGTCCAAGGACTTCGATTTTCG  
 AAAAGACCGAGATGAAGTACGACTCGACCGGCATGTTCCACTGGTCCCCAGCTAAGTCTCTCGAGGATTGCATCTTGGAC  
 CGTAACCAGGCTGCTATGACCGTGTGTAACGGTCACGTGGTGTGCTGCTCTTCGCTGACCTGACTCTCCTCTGATCGG  
 ACTGCGTAACCTGGTCATGCCTCTGCGCGCTTCTAACTTCCACTACCACGAAGTGAAGCACGTGGTCATCGTGGGTTCCG  
 TGGACTACATCCGTGCGAGTGGAAGATGCTGCAGAACCTGCCTAAGATCTCCGTGCTGAACGGCTCCCCCTCTGTCTCGT  
 GCTGATCTGCGTGTGTGAACGTGAACCTGTGCGACATGTGCTGCATCCTGTCCGCTAAGGTGCCATCCAACGACGATCC  
 CACTCTGGCTGACAAAGAGGCTATCCTGGCTTCCCTCAACATCAAGGCTATGACCTTCGACGACACCATCGGCGTGTGT  
 CTCAACGTGGTCCCGAGTTCGACAACCTGTCTGCTACCGCTGGTTCCCTATCGTGCTGCAACGTGCTGGTTCCGTCTAC  
 GGTGCTAACGTGCCCATGATCACCGAGCTGGTCAACGACGGCAACGTCCAGTTCTTGGACCAGGACGACGACGATGACCC  
 CGACACCGAACTGTACCTGACTCAGCCTTTCGCTTGGCGCACCGCTTTCGCTGTGTCTGTCTGGACTCCCTGATGTCCA  
 CCACCTACTTCAACCAGAATGCTCTGACCCTCATCCGTCTCTGATCACCGGTGGCGCTACCCCTGAGCTGGAAGTATGATC  
 TTGGCTGAAGGCGCTGGACTGCGCGGTGGTTACTCTACTGTGGAATCCCTGTCCAACCGCAGCGTTGCCGTGTGGGTCA  
 AATCTCCTTGTACGACGTTCCCTGGCTCAGTTCGGAGAGTGTGGCAAATACGGCGACCTGTTTCGTGGCTGCTCTGAAGT  
 CCTACGGCATGCTGTGATCGGCCTGTACCGTTTCCGTGACACCTCTTCTCTTTCGACGCTCCTCCAAGCGTTACGTC  
 ATCACTAACCACCTGACGACTTCTCCCTGCTGCCTACCGACCAAGTGTTCGTGCTCATGAGTTTCGACCCCGGCTCGA  
 GTACAAGCCTCCTGCTGTAGGGCTCCAGCTGGTGGTGTGGCACCAATACTCAAGGTTCCGGTGTGCTGGTGGCGGTT  
 CCAACAAGGACGACAACCTCCGGTTCCTCTGGAAACCGAGACTTCCCAAGTGGCTCCCGCTTAA

The sequences corresponding to the GSSG linker, the Rho1D4 and the Stop codon are highlighted in cyan, yellow and red, respectively.



**Supplementary Table 2. Cryo-EM data collection, refinement and validation statistics**

	Ca <sup>2+</sup> -bound Slo (EMDB- 13700) (PDB 7PXE)	Ca <sup>2+</sup> -free Slo (EMDB- 13701) (PDB 7PXF)	Slo- Verruculogen (EMDB-13702) (PDB 7PXG)	Slo- Emodepside (EMDB-13703) (PDB 7PXH)
<b>Data collection and processing</b>				
Magnification			130,000	
Voltage (kV)			300	
Electron exposure (e-/Å <sup>2</sup> )	74.0	79.8	80.4	75.4
Defocus range (µm)			-0.9 to -2.1	
Pixel size (Å)		0.35 (super-resolution) / 0.70 (native)		
Symmetry imposed	C4	C4	C4	C2
Initial particle images (no.)	906,619	920,897	1,131,410	1,861,584
Final particle images (no.)	225,754	90,833	66,077	261,505
Map resolution (Å)	2.38	2.68	2.73	2.59
FSC threshold	0.143	0.143	0.143	0.143
Map resolution range (Å)	2.0 – 3.1	2.4 – 3.8	2.4 – 4.0	2.2 – 3.4
<b>Refinement</b>				
Initial model used (PDB code)		Homology model based on PDB 5TJ6 ( <a href="https://doi.org/10.2210/pdb5TJ6/pdb">https://doi.org/10.2210/pdb5TJ6/pdb</a> )		
Model resolution (Å)	2.5	2.9	2.9	2.7
FSC threshold	0.5	0.5	0.5	0.5
Map sharpening <i>B</i> factor (Å <sup>2</sup> )	33.8	26.1	23.8	36.3
Model composition				
Non-hydrogen atoms	28,928	28,099	28,664	28,923
Protein residues	3,540	3,540	3,540	3,540
Ligands	700	7	572	829
Water	136	-	-	2
<i>B</i> factors (Å <sup>2</sup> )				
Protein	83.8	102.8	74.2	82.4
Ligand	106.2	84.3	87.5	104.8
Water	67.8	-	-	83.2
R.m.s. deviations				
Bond lengths (Å)	0.002	0.002	0.002	0.002
Bond angles (°)	0.390	0.446	0.483	0.430
Validation				
MolProbity score	1.51	1.32	1.37	1.19
Clashscore	5.34	5.57	6.51	4.03
Poor rotamers (%)	1.94	0.65	1.03	0.26
Ramachandran plot				
Favored (%)	99.0	97.9	98.6	98.2
Allowed (%)	1.0	2.1	1.4	1.8
Disallowed (%)	0.0	0.0	0.0	0.0